

Activated Methane on Small Cationic Platinum Clusters**

Dan J. Harding, Christian Kerpal, Gerard Meijer and André Fielicke*

The catalytic activation of C-H bonds in small hydrocarbons, particularly methane, is a reaction which is of significant technological interest, as it allows valuable, functionalized products to be made from plentiful, cheap feedstocks. However, even on well characterized platinum surfaces determination of the details of methane activation, in particular the earliest steps, remains difficult. [1, 2] Challenges include the weak physisorption of molecular methane on platinum surfaces, its ready dissociation and the difficulty associated with determining H atom positions in many surface experiments, as H atoms are weak scatterers of X-rays or electrons and have no electronic core levels. [3] Despite these challenges, Yoshinobu *et al.* have used infrared reflection absorption spectroscopy to show that CH₄ adsorbed on Pt(111) has at most C_{3v} symmetry. [4] Öström *et al.* have determined the adsorption geometry of methane on Pt(977) [5] using X-ray absorption spectroscopy, reporting methane to bind via a single H atom, though they were unable to determine whether it was bound atop or in hollow sites. Partially dehydrogenated reaction intermediates/products including methyl, methylene and methylidyne have been extensively studied (see for example [6]).

The reactions of methane with platinum atoms and clusters have been studied in some detail. [7] In the case of small ionic clusters reacting with CH₄ under single collision conditions Pt_n[C,2H]⁺ complexes were found to be the favored products. [8–10] There have been a number of computational studies of the interactions of platinum clusters [11–13] and surfaces [5, 14, 15] with methane, primarily using density functional theory (DFT). Such calculations are challenging, due to the large system size, number of electrons and possible paths, and the fact that several electronic states and crossings between them may need to be treated. [13] Experimental spectroscopic characterization of these species, particularly the reaction intermedi-

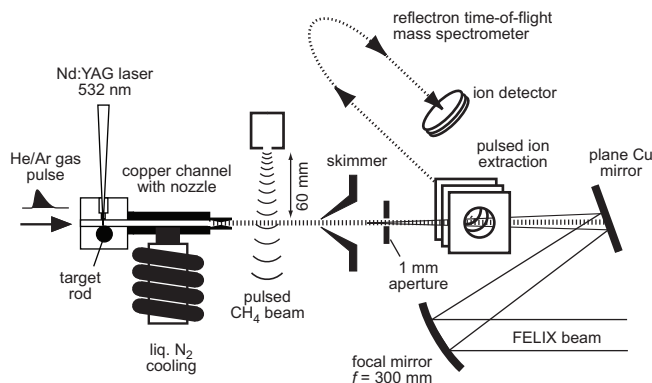
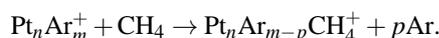


Figure 1: The crossed-beam experimental setup.

ates, can therefore provide important information about their structures and benchmark data for theory.

Recently, we have demonstrated the possibility of forming reactive intermediate species under thermalized conditions in a flow reactor. [16] This approach was unsuccessful for the Pt_n⁺-CH₄ system due to rapid dehydrogenation of the CH₄, apparently occurring in the metal plasma generated during the laser ablation process. Here, we use a different method to stabilize complexes along the entrance channel of the gas-phase reactions, specifically Pt_{3–5}CH₄⁺, which allows their spectroscopic characterization. This is achieved by ligand exchange between CH₄ and Ar on cold pre-formed Pt_nAr_m⁺ complexes:



The modified experimental setup is shown in Fig 1. Platinum clusters are formed by laser ablation from an isotopically enriched ¹⁹⁴Pt target. Adding 0.2 % Ar to the He carrier gas and cooling the thermalization channel to 180 K yields a distribution (without CH₄) of clusters Pt_nAr_{0–5}⁺. For experimental details see Ref. [17]. After expansion from the source the cluster beam is crossed by a molecular beam of CH₄ from a pulsed valve. The reaction products are analyzed in a time-of-flight mass spectrometer. Under these (near-)single-collision conditions formation of Pt_nCH₄Ar_{0–4}⁺ complexes is observed. The adsorption energy must be efficiently removed by the evaporating Ar atoms, quenching the complex into an early local minimum on the dehydrogenation reaction pathway. Pt_n⁺ clusters without Ar ligands form primarily Pt_nCH₂⁺ complexes, in

[*] Dr. D. J. Harding, C. Kerpal, Prof. Dr. G. Meijer, Dr. A. Fielicke Fritz-Haber-Institut der Max-Planck-Gesellschaft, Faradayweg 4-6, 14195 Berlin, Germany

E-mail: fielicke@fhi-berlin.mpg.de

[**] We gratefully acknowledge the support of the Stichting voor Fundamenteel Onderzoek der Materie (FOM) for providing FELIX beam time and the FELIX staff, in particular Dr. B. Redlich and Dr. A.F.G. van der Meer, for their skillful assistance. This work is supported by the Deutsche Forschungsgemeinschaft through research grant FI893/3-1. DJH thanks the Alexander-von-Humboldt-Stiftung for support.

Supporting Information is available for this article on the WWW under <http://>

agreement with earlier experiments under single collision conditions. [8–10] Similar changes in reactivity with argon coverage, from rapid dehydrogenation to sticking of CH₄, have been observed for Pt⁺ atomic ions. [18] The Ar coverage dependence of the reactions of Rh_nAr_m⁺ with methane has been investigated in detail, [19] showing the formation of Rh_n[C,4H]⁺ and Rh_n[C,2H]⁺ complexes, while most bare Rh_n⁺ clusters (except Rh₂⁺) are essentially unreactive towards methane. Mass spectrometry alone cannot, however, provide detailed information about the structures of the complexes.

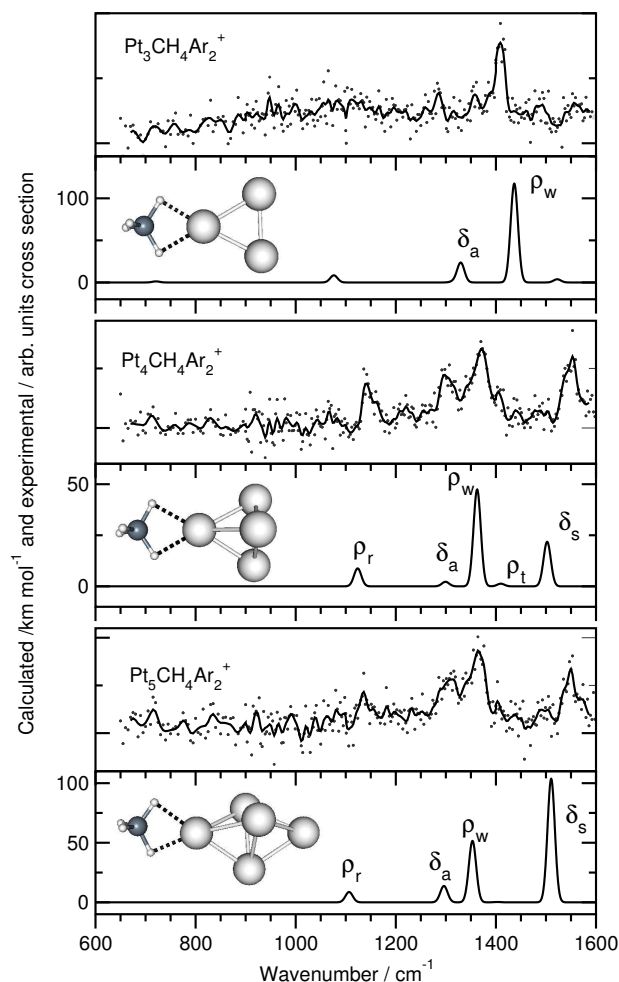


Figure 2: Experimental IR-MPD spectra of Pt_nCH₄Ar₂⁺ ($n=3-5$), monitored by depletion of the parent ion signal in all cases. The most intense peaks correspond to a decrease of approximately 60% in the parent signal. The experimental data (grey points) are smoothed with a 9-point binomial average. The calculated structures and spectra, with assignments, which provide the best match to the experiment are shown for the Pt_nCH₄⁺ complexes. The calculated vibrational frequencies are scaled by a factor of 0.97.

In the present study, experimental vibrational spectra of Pt_nCH₄Ar₁₋₄⁺ complexes are obtained between 650 and 1600 cm⁻¹ by infrared multiple photon dissociation (IR-MPD), using the Free Electron Laser for Infrared eXperiments (FELIX). [20] This range covers the characteristic C-H deformation modes of CH₂,

CH₃ and CH₄ species. To aid in the structural identification we have also performed DFT calculations on a range of Pt_n[C,4H]⁺ species at the TPSS/def2-TZVP level of theory [21] using TURBOMOLE. [22] The initial structures for the platinum clusters were low-energy geometries and spin multiplicities that we have identified from a combined IR-MPD and computational study of the small bare Pt clusters. [23] IR-MPD spectra and the best-matching calculated spectra are shown in Figure 2. The modes are assigned based on the motion of the non-bonding H atoms. A range of alternative structures including partially dehydrogenated, η₁-CH₄ and η₃-CH₄ complexes were also considered, but provide less good matches to the experimental spectra, examples are shown in the Supplementary Information.

The experimental spectra of the [C,4H] complexes have features in the range 1140–1560 cm⁻¹, consistent with symmetry induced splitting of the *e* (1534 cm⁻¹) and *t*₂ (1306 cm⁻¹) vibrational modes of free methane. The broad splitting, particularly for $n=4,5$ suggests a significant degree of activation of the C-H bonds in the complexes. For $n=3$ the calculated spectrum which best matches the experimental spectrum is not that of the lowest-energy isomer we have found, a partially dehydrogenated species, but of molecularly adsorbed η₂-CH₄, bound by two H atoms to one Pt atom in the cluster. For $n=4$, the molecularly bound species is the lowest-energy structure we have found, while for $n=5$, molecularly and dissociatively adsorbed species are essentially isoenergetic. In both cases, η₂-CH₄ molecularly adsorbed species provide the best matches to the experimental spectra. In the trigonal bipyramid Pt₅⁺ there are two distinct types of Pt atom, *i.e.* 3- and 4-coordinate, to which the CH₄ can bind. The calculated total energies in these sites differ (CH₄ on a 4-coordinate Pt atom is 0.29 eV higher in energy) but the calculated frequencies and relative intensities are rather similar, making it difficult to determine which site is favored.

Overall, the agreement between theory and experiment is good for $n=4,5$, matching the number, position and relative intensities of the bands. The agreement for Pt₃CH₄⁺ is less good than for the larger clusters, but a similar blue-shift of the intense ρ_w feature around 1400 cm⁻¹ is observed in both the experimental and calculated spectra. The structures we identify are similar to those predicted for Pt₃CH₄⁺ [11] and Pt₄CH₄⁺. [13]

In order to investigate the degree of activation of the C-H bonds in the complexes we have compared the changes of the C-H bondlengths with those of small hydrocarbons. The most activated, tertiary, C-H bond in *iso*-butane has a bond length of 1.122 Å while free CH₄ has bond lengths of 1.087 Å, a change of the order of 0.03 Å. [24] The most activated bonds in the $n = 3, 4, 5$ complexes are calculated to be 1.15 Å, 1.13 Å and 1.14 Å respectively, while the 'unactivated' bonds and free CH₄ are all 1.09 Å. Such elongation, up to 0.06 Å, of the C-H bonds in the complex demonstrates

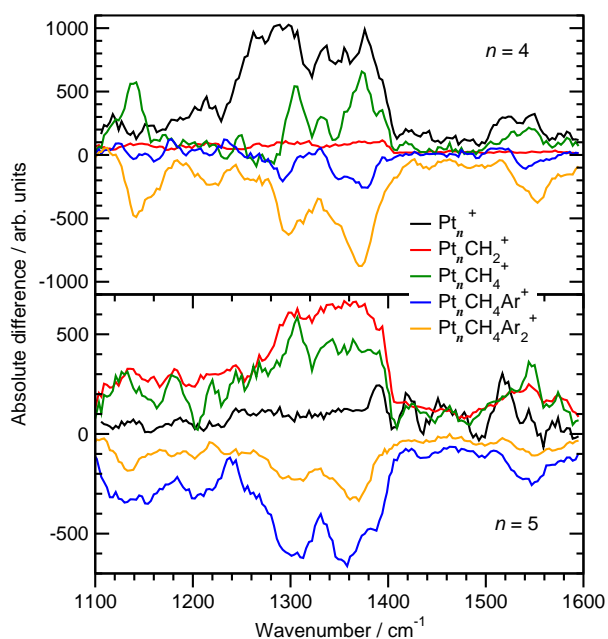


Figure 3: Absolute differences in mass spectrometric intensity following IR-MPD for 4 and 5 atom Pt clusters.

that the methane is highly activated. For comparison, Öström *et al.* [5] found the η_1 -CH₄ on Pt(977) to have a bond length of 1.18 ± 0.05 Å. The Pt-CH₄ binding fits into the picture of an agostic bond, with interaction between a filled C-H sp^3 orbital and a Pt d orbital. [13, 14, 25]

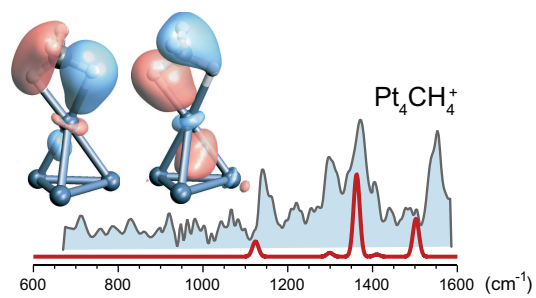
The dissociation channels for the different cluster sizes after IR excitation can also provide useful information. Fig. 3 shows the changes in mass spectral intensity for the important species involved in the IR-MPD process for $n=4,5$. For the Pt_{3,5}⁺ complexes, we observe growth (corresponding to the depletion of the Ar complexes) primarily in the Pt_{3,5}CH₂⁺ and Pt_{3,5}CH₄⁺ channels, showing that the IR excitation can drive the partial dehydrogenation reaction in competition with dissociation by loss of Ar or CH₄. In contrast, for Pt₄⁺ growth in the Pt₄CH₂⁺ channel is not observed, indicating that the rate of IR-induced dehydrogenation is lower than the rates of Ar or CH₄ boil-off. This low observed reactivity of Pt₄⁺ is consistent with previous studies [8–10] but suggests that, in addition to the lack of thermodynamic driving force reported by Koszinowski *et al.* [9], there may also be a larger barrier to partial dehydrogenation on Pt₄⁺ than on the other cluster sizes. The suggestion that the barrier to dehydrogenation on Pt₄⁺ is higher than that for CH₄ desorption is consistent with the calculations of Lv *et al.*, who reported the transition state (TS) for Pt₄⁺ insertion into a C-H bond to be higher in energy than the separated species, in contrast to Pt₃⁺ where this TS lies slightly lower in energy than the separated molecules. Entropic factors may also be important, given that the number of pathways for dissociation are presumably much greater than for dehydrogenation.

The structures we have identified for methane adsorbed on small clusters have different binding geometries to those identified on extended platinum surfaces. [5] Despite this, the dehydrogenation reaction pathways appear to be similar, and our findings support the model of De Witt *et al.* in which dissociative adsorption of methane on Pt proceeds via a shallow minimum with similar barriers to dehydrogenation and desorption. [2] The experimental dissociation channels and calculated C-H bond activation correlate well with the results of previous FT-ICR reactivity studies, with Pt₄⁺ showing less activation and much lower activity for dehydrogenation. The observation that the C-H bond activation is distributed over two bonds on the cluster, with a corresponding reduction in the degree of activation of each bond, may explain the previously noted reduced activity of supported Pt nanoclusters compared to extended Pt surfaces. [2] This reduced activation may, however, be an advantage, allowing greater control over the reactivity of methane on nanostructured catalysts.

References

- [1] T. V. Choudray, E. Aksoylu, D. W. Goodman, *Catal. Rev.* **2003**, *45*, 151–203. A. L. Marsh, K. A. Becraft, G. A. Somorjai, *J. Phys. Chem. B.* **2005**, *109*, 13619–13622. H. Schwarz, *Angew. Chem. Int. Ed.* **2011**, *50*, 10096–10115. *Angew. Chem.* **2011**, *123*, 10276–10297.
- [2] K. M. DeWitt, L. Valadez, H. L. Abbott, K. W. Kolasinski, I. Harrison, *J. Phys. Chem. B* **2006**, *110*, 6705–6713.
- [3] D. P. Woodruff, *Chem. Soc. Rev.* **2008**, *37*, 2262–2273.
- [4] J. Yoshinobu, H. Ogasawara, M. Kawai, *Phys. Rev. Lett.* **1995**, *75*, 2176–2179.
- [5] H. Öström, H. Ogasawara, L.-Å. Näslund, L. G. M. Pettersson, A. Nilsson, *Phys. Rev. Lett.* **2006**, *96*, 146104. H. Öström, H. Ogasawara, L.-Å. Näslund, K. Andersson, L. G. M. Pettersson, A. Nilsson, *J. Chem. Phys.* **2007**, *127*, 144702.
- [6] C. Papp, T. Fuhrmann, B. Tränkenschuh, R. De-necke, H.-P. Steinrück, *Chem. Phys. Lett.* **2007**, *442*, 176–181.
- [7] C. Heinemann, R. Wesendrup, H. Schwarz, *Chem. Phys. Lett.* **1995**, *239*, 75–83. X.-G. Zhang, R. Liyanage, P. B. Armentrout, *J. Am. Chem. Soc.* **2001**, *123*, 5563–5575. H.-G. Cho, L. Andrews, *J. Phys. Chem. A* **2008**, *112*, 12293–12295. D. J. Trevor, D. M. Cox, A. Kaldor, *J. Am. Chem. Soc.* **1990**, *112*, 3742–3749.
- [8] U. Achatz, C. Berg, S. Joos, B. S. Fox, M. K. Beyer, G. Niedner-Schatteburg, V. E. Bondybey,

- Chem. Phys. Lett.* **2000**, *320*, 53–58. T. Hanmura, M. Ichihashi, T. Kondow, *J. Phys. Chem. A* **2002**, *106*, 11465–11469.
- [9] K. Koszinowski, D. Schröder, H. Schwarz, *J. Phys. Chem. A* **2003**, *107*, 4999–5006.
- [10] G. Kummerlöwe, I. Balteanu, Z. Sun, O. P. Balaj, V. E. Bondybey, M. K. Beyer, *Int. J. Mass Spectrom.* **2006**, *254*, 183. C. Adlhart, E. Uggerud, *Chem. Commun.* **2006**, 2581–2582. C. Adlhart, E. Uggerud, *Chem. Eur. J.* **2007**, *13*, 6883–6889.
- [11] H. Basch, D. G. Musaev, K. Morokuma, *J. Mol. Struct. THEOCHEM* **2002**, *586*, 35–46.
- [12] L. Xiao, L. Wang, *J. Phys. Chem. B* **2007**, *111*, 1657–1663. F. Xia, Z. Cao, *J. Phys. Chem. A* **2006**, *110*, 10078–10083.
- [13] L. Lv, Y. Wang, Q. Wang, H. Liu, *J. Phys. Chem. C* **2010**, *114*, 17610–17620.
- [14] J.-Y. Saillard, R. Hoffmann, *J. Am. Chem. Soc.* **1983**, *106*, 2006–2026.
- [15] F. Viñes, Y. Lykhach, T. Staudt, M. Lorenz, C. Papp, H. Steinrück, J. Libuda, K. Neyman, A. Görling, *Chem. Eur. J.* **2010**, *16*, 6530–6539.
- [16] S. M. Hamilton, W. S. Hopkins, D. J. Harding, T. R. Walsh, P. Gruene, M. Haertelt, A. Fielicke, G. Meijer, S. R. Mackenzie, *J. Am. Chem. Soc.* **2010**, *132*, 1448–1449. S. M. Hamilton, W. S. Hopkins, D. J. Harding, T. R. Walsh, M. Haertelt, C. Kerpel, P. Gruene, G. Meijer, A. Fielicke, S. R. Mackenzie, *J. Phys. Chem A* **2011**, *115*, 2489–2497.
- [17] A. Fielicke, G. von Helden, G. Meijer, *Eur. Phys. J. D* **2005**, *34*, 83–88.
- [18] U. Achatz, M. Beyer, S. Joos, B. S. Fox, G. Niedner-Schatteburg, V. E. Bondybey, *J. Phys. Chem. A* **1999**, *103*, 8200–8206.
- [19] G. Albert, C. Berg, M. K. Beyer, U. Achatz, S. Joos, G. Niedner-Schatteburg, V. E. Bondybey, *Chem. Phys. Lett.* **1997**, *268*, 235–241.
- [20] D. Oepts, A. F. G. van der Meer, P. W. van Amersfoort, *Infrared Phys. Technol.* **1995**, *36*, 297–308.
- [21] J. Tao, J. P. Perdew, V. N. Staroverov, G. E. Scuseria, *Phys. Rev. Lett.* **2003**, *91*, 146401. D. Andrae, U. Häußerman, M. Dolg, H. Stoll, H. Preuß, *Theor. Chim. Acta* **1990**, *77*, 123. F. Weigend, M. Häser, H. Patzelt, R. Ahlrichs, *Chem. Phys. Lett.* **1998**, *294*, 143–152. F. Weigend, R. Ahlrichs, *Phys. Chem. Chem. Phys.* **2005**, *7*, 3297–3305.
- [22] R. Ahlrichs, M. Bär, M. Häser, H. Horn, C. Kölmel, *Chem. Phys. Lett.* **1989**, *162*, 165–169.
- [23] D. J. Harding, C. Kerpel, D. M. Rayner, G. Meijer, A. Fielicke, *in preparation*.
- [24] D. R. Lide (Ed.), *CRC Handbook of Chemistry and Physics*, CRC Press, Boca Raton, **1995**.
- [25] M. Brookhart, M. L. H. Green, G. Parkin, *Proc. Nat. Acad. Sci. USA* **2007**, *104*, 6908–6914.
- [26] K. Eichkorn, O. Treutler, H. Oehm, M. Haeser, R. Ahlrichs, *Chem. Phys. Lett.* **1995**, *240*, 183.
- [27] K. Eichkorn, F. Weigend, O. Treutler, R. Ahlrichs, *Theo. Chem. Acc.* **1997**, *97*, 119.



StretC-H Me-H: Methane activated by adsorption on small platinum clusters is characterized by the vibrational fingerprint of the cluster complex.

Keywords: C-H bond activation, clusters, molecular beams, platinum, vibrational spectroscopy

Supporting Information

Computational Details

Density functional theory (DFT) calculations have been carried out in an effort to determine the low-energy structures of the $Pt_nCH_4^+$ clusters and to provide calculated IR spectra for comparison with the experimental results. The calculations were performed using TURBOMOLE v6.0. [22] with the TPSS exchange-correlation functional [21] and def2-TZVP ECP (for Pt) and basis sets. [] The resolution of the identity approximation (RIJ) was used to speed up the calculations. [26, 27] Harmonic spectra were calculated analytically, the frequencies were scaled by a factor of 0.97, after comparison between experiment and theory. The stick spectra were convoluted with a Gaussian line-shape function of full width at half maximum height of 20 cm^{-1} to aid comparison with experiment. The initial structures used for the bare platinum clusters were low-energy geometries and spin multiplicities that we have identified from a combined IR-MPD and computational study of the small bare Pt clusters. [23] A range of different input geometries and spin multiplicities were considered for local optimization for the $Pt_nCH_4^+$ complexes, including various molecular adsorption sites and geometries (η_1, η_2, η_3), and partial dehydrogenation (methyl and methylene plus H atom(s)). The η_1 and η_3 binding geometries were unstable, collapsing to η_2 during optimization. The spectra and relative energies for a range of the structures we found are shown below. As the complexes in the experiment are formed in a way in which kinetic control may be more important than energetic factors, it is not surprising that lowest-energy structures we found in the calculations are not always those that we identify spectroscopically.

$Pt_3CH_4^+$ spectra

Figure 4 shows calculated structures, relative energies and spectra for several isomers of $Pt_3CH_4^+$. The two lowest-energy structures are both insertion complexes, with CH_3 groups. In the region covered by our experimental measurements their spectra are rather similar, except for the intense band at 973 cm^{-1} due to the bridge-bound H-atom for isomer 3-4. Neither spectrum provides a good match to the experiment. The two isomers with intact CH_4 are 0.4 eV higher in energy, but provide a much better match to experiment. Isomer 3-9 provides probably the best match, but 3-11 would also fit reasonably well, especially if the frequencies are not scaled.

$Pt_4CH_4^+$ spectra

For $Pt_4CH_4^+$, shown in Fig. 5, the lowest energy structure we have found is the η_2 , whose spectrum best matches the experiment. The insertion complexes are higher in energy by $0.4\text{--}0.5\text{ eV}$. The most intense bands

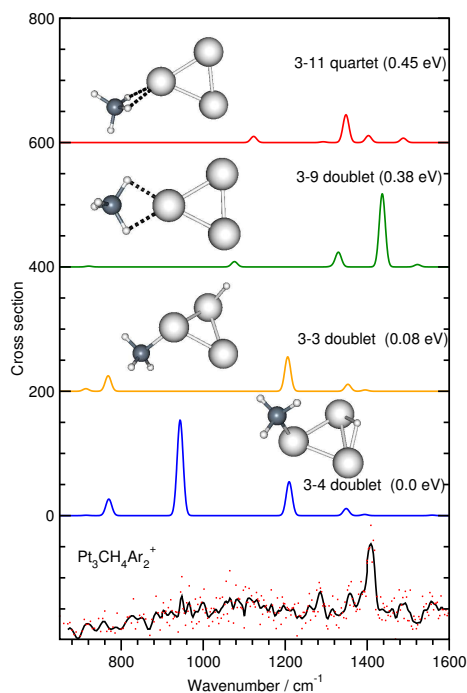


Figure 4: Comparison of the experimental spectrum of $Pt_3CH_4Ar_2^+$ and calculated spectra for some isomers of $Pt_3CH_4^+$. The calculated cross sections are in km mol^{-1} , offset for clarity. The experimental spectrum is in arbitrary units. The calculated structures, spin multiplicities and relative energies are also shown.

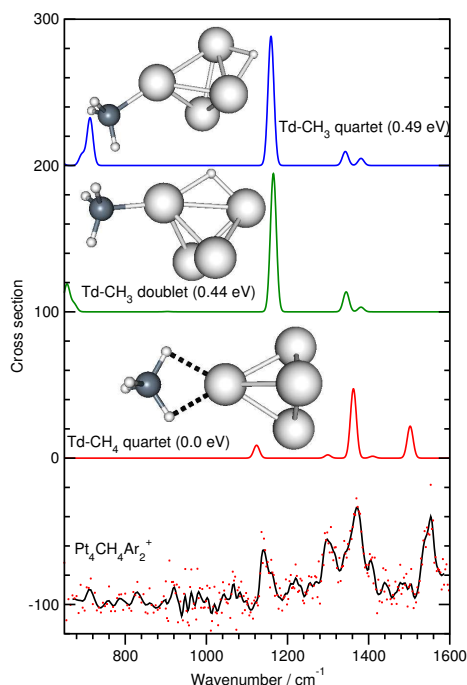


Figure 5: Comparison of the experimental spectrum of $Pt_4CH_4Ar_2^+$ and calculated spectra for some isomers of $Pt_4CH_4^+$. The calculated cross sections are in km mol^{-1} , offset for clarity. The experimental spectrum is in arbitrary units. The calculated structures, spin multiplicities and relative energies are also shown.

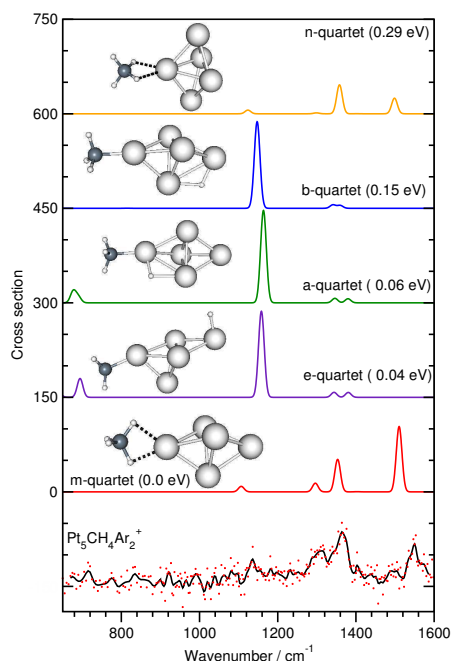


Figure 6: Comparison of the experimental spectrum of $\text{Pt}_5\text{CH}_4\text{Ar}_2^+$ and calculated spectra for some isomers of Pt_5CH_4^+ . The calculated cross sections are in km mol^{-1} , offset for clarity. The experimental spectrum is in arbitrary units. The calculated structures, spin multiplicities and relative energies are also shown.

for these isomers are at *ca.* 1160 cm^{-1} while they do not have features at 1550 cm^{-1} , making them a poor match to the experimental spectrum.

Pt_5CH_4^+ spectra

We have found several isomers of Pt_5CH_4^+ which lie very close in energy. These include the η_2 molecularly adsorbed complex bound to a 3-coordinate Pt (isomer **m**) and several insertion complexes (isomers **e**, **a**, and **b**), their structures, spin multiplicities, calculated spectra and relative energies are shown in Fig. 6. We also show the calculated spectrum of the η_2 molecularly adsorbed complex bound to a 4-coordinate Pt (isomer **n**), which is higher in energy. Again, the insertion complexes do not provide a good match to the experimental spectrum, with intense bands at *ca.* 1150 cm^{-1} . Both of the molecularly adsorbed species provide good matches to the experiment, the significantly lower energy of isomer **m** leads us to suggest it is this one which is likely to dominate the experimental population. (Though there are more 4-coord. Pt atoms, which might favor isomer **n**.)

Cartesian Coordinates

Cartesian coordinates, in Ångstroms, of the cluster structures discussed here.

8
3-4 2tet Energy = -398.2755272765
Pt -1.3826670 -0.1803833 0.0000000
Pt 0.7767930 0.0231692 1.2905785
Pt 0.7767930 0.0231692 -1.2905785
C -2.2625676 1.6143499 0.0000000
H -2.8712645 1.6004602 -0.9151984
H -2.8712645 1.6004602 0.9151984
H -1.5481839 2.4371948 0.0000000
H 1.1726288 1.0677015 0.0000000
8
3-3 2tet Energy = -398.2726303224
Pt 0.3741169 -1.3542971 -0.1810092
Pt 0.9848942 1.1381061 0.0407459
Pt -1.4013181 0.3835651 0.0189745
C 0.4779733 -2.2297179 1.6180323
H -0.0904641 -3.1590804 1.4666049
H 1.5469488 -2.4130248 1.7850500
H 0.0411749 -1.6174030 2.4073919
H 0.9947334 1.3660559 -1.4658750
8
3-9 2tet Energy = -398.2614758899
Pt 0.0253779 1.3641084 -0.0002729
Pt -1.2015508 -0.8102021 0.0000129
Pt 1.1776683 -0.8515156 0.0001194
C -0.0169270 3.6175481 0.0009302
H -0.0905656 4.2062813 -0.9130045
H -0.0014068 4.2272036 0.9044184
H 0.9849019 3.0670853 -0.0406272
H -0.9806336 2.9906655 0.0653503
8
3-11 4tet Energy = -398.2591295291
Pt 0.1701912 1.3645617 -0.0094121
Pt 1.1616244 -0.8865170 0.0043255
Pt -1.2787719 -0.7711660 0.0003129
C -0.6397233 3.5638830 0.0565061
H 0.1061958 4.3580427 0.0526528
H -1.6613457 3.9399845 0.1294743
H -0.4959467 2.9463811 0.9988071
H -0.5918030 3.0177081 -0.9303888
9
td-4tet-ch4 Energy = -517.6645976030
Pt 0.0167337 0.2353471 1.5014472
Pt 1.2116295 0.7451516 -0.7266212
Pt 0.1011217 -1.5345070 -0.4089617
Pt -1.3261947 0.5674737 -0.6811186
C -0.0225068 -0.1641491 3.8264298
H -0.1599954 0.6595025 4.5265785
H 0.0463542 -1.1333991 4.3205352
H -0.9571201 -0.2168779 3.1875098
H 0.9648567 -0.0071184 3.3067900
9
td-CH3-bridge2 2tet E = -517.6483673317
Pt 0.7974332 1.3486067 -0.0102415
Pt -0.9240853 -0.0413055 1.2619499
Pt -0.8437190 -0.1364505 -1.3168083
Pt 0.9299108 -1.4316892 0.0690739
C 0.4029386 3.3289768 -0.0553775

H	0.8618224	3.7312144	0.8581254	C	0.0951484	4.1218748	0.0767723
H	0.9036745	3.6916085	-0.9643731	H	0.6087064	4.3974672	1.0101058
H	1.9286935	-0.1615733	0.0830275	H	0.6774005	4.4607338	-0.7874353
H	-0.6650997	3.5521167	-0.0860165	H	1.5487704	-1.8087156	0.0937019
9				H	-0.9231425	4.5239491	0.0506589
td-CH3-bridge1 4tet E = -517.6466866860				10			
Pt	-1.3707286	-0.0679065	0.7243164	n-4tet Energy = -637.0191189414			
Pt	0.2755799	-1.3556606	-0.7546630	Pt	0.0000669	-0.1079865	-2.1437792
Pt	0.0039617	1.2004483	-0.9974222	Pt	0.0001373	-0.1128260	2.1433665
Pt	1.3467616	0.2237287	0.9900653	Pt	1.2930047	-0.7822299	-0.0008526
C	-3.3770681	0.0550478	0.4862789	Pt	-1.2891391	-0.7886986	-0.0007488
H	-3.7785314	-0.7846082	1.0714141	Pt	-0.0043740	1.4751265	-0.0005608
H	-3.6486714	1.0206397	0.9370170	C	0.0036361	3.8479040	0.0316671
H	1.9045263	-1.0184939	0.0484989	H	0.9661309	3.2583513	-0.0080967
H	-3.6988413	0.0084664	-0.5544789	H	-0.0122180	4.4739354	-0.8602998
10				H	-0.9647641	3.2674763	0.0336044
m-4tet Energy = -637.0299489430				H	0.0263778	4.4247031	0.9558046
Pt	-0.0002147	-2.2225093	0.0035457				
Pt	0.0058440	2.0933678	-0.0279528				
Pt	-1.3248934	-0.0816049	0.6826399				
Pt	0.0733497	-0.0700796	-1.4893605				
Pt	1.2492640	-0.0808297	0.8121236				
C	-0.0407061	4.3952349	0.2337903				
H	0.0091439	3.7526188	1.1554291				
H	0.8569214	5.0130288	0.2271136				
H	-0.0659721	3.8822765	-0.7848108				
H	-0.9632854	4.9716203	0.2943798				
10							
e-4tet Energy = -637.0283297998							
Pt	-0.0422000	-2.5687113	0.0028629				
Pt	-0.5271879	1.9497077	0.6084033				
Pt	0.7779628	-0.3490172	1.0669824				
Pt	-1.1710713	-0.3089577	-0.5781374				
Pt	1.0120506	0.9808735	-1.1443836				
C	-0.5709789	3.9661091	0.4946951				
H	0.2840596	4.3272203	1.0781534				
H	-0.5319068	4.3257291	-0.5347548				
H	-1.0108504	-2.8253902	1.1531993				
H	-1.5280097	4.2189956	0.9768989				
10							
a-4tet Energy = -637.0279261621							
Pt	-0.0040714	-2.2460262	0.0041389				
Pt	-0.0438769	2.1984740	-0.0022340				
Pt	-0.7541098	-0.0976746	1.2726539				
Pt	-0.7021022	-0.1059416	-1.3045726				
Pt	1.4831973	-0.0886551	0.0292664				
C	0.1683037	4.2147054	0.0079484				
H	0.7653349	4.5274771	0.8685415				
H	0.6260266	4.5310142	-0.9338523				
H	1.5282698	1.9085921	0.0249602				
H	-0.8680505	4.5783244	0.0902808				
10							
b-4tet Energy = -637.0243158233							
Pt	0.0227662	-2.3221055	-0.0078155				
Pt	-0.0987350	2.1081858	-0.0080732				
Pt	-0.8215620	-0.1046004	1.2177357				
Pt	-0.6253321	-0.0703906	-1.3223071				
Pt	1.5071267	0.0753259	0.1138367				